

AD-A082 384

AIR FORCE GEOPHYSICS LAB HANSCOM AFB MA
DEVELOPMENT AND EVALUATION OF A TOWER SLANT VISUAL RANGE SYSTEM--ETC(U)
SEP 79 E B GEISLER

F/G 1/2

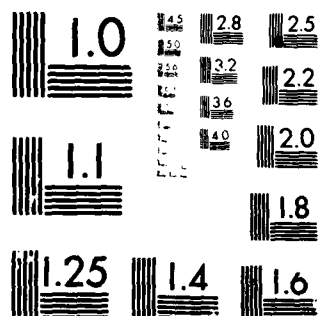
UNCLASSIFIED

AFGL-TR-79-0209

NL

1 G-1
ALL INFORMATION
CONTAINED
HEREIN IS UNCLASSIFIED

END
DATE
FILMED
4-80
DTIC



MICROCOPY RESOLUTION TEST CHART
NATIONAL BUREAU OF STANDARDS-1963-A

AD A 082384

AFOL-TR-79-0209
INSTRUMENTATION PAPERS, NO. 281

(12)
A

LEVEL



Development and Evaluation of a Tower Slant Visual Range System

EDWARD B. GEISLER, Capt, USAF

14 September 1979

Approved for public release; distribution unlimited.

DTIC
ELECTE
MAR 27 1980
S D A

METEOROLOGY DIVISION PROJECT 6670
AIR FORCE GEOPHYSICS LABORATORY
HANSCOM AFB, MASSACHUSETTS 01731

AIR FORCE SYSTEMS COMMAND, USAF



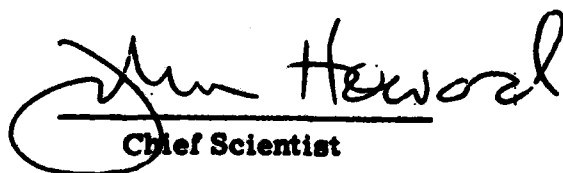
80 3 26 083

DDC FILE COPY

This report has been reviewed by the ESD Information Office (OI) and is releasable to the National Technical Information Service (NTIS).

This technical report has been reviewed and is approved for publication.

FOR THE COMMANDER


Chief Scientist

Qualified requestors may obtain additional copies from the Defense Documentation Center. All others should apply to the National Technical Information Service.

⑨ Instrumentation

Unclassified

SECURITY CLASSIFICATION OF THIS PAGE (When Data Entered)

REPORT DOCUMENTATION PAGE		READ INSTRUCTIONS BEFORE COMPLETING FORM	
1. REPORT NUMBER	2. GOVT ACCESSION NO.	3. RECIPIENT'S CATALOG NUMBER	
14 AFGL-TR-79-8209, AFGL-IP-281			
4. TITLE (and Subtitle)		5. TYPE OF REPORT & PERIOD COVERED	
6 DEVELOPMENT AND EVALUATION OF A TOWER SLANT VISUAL RANGE SYSTEM		Scientific. Interim.	
7. AUTHOR(s)		6. PERFORMING ORG. REPORT NUMBER	
10 Edward B. Geisler Capt, USAF		IP No. 281	
8. PERFORMING ORGANIZATION NAME AND ADDRESS		9. CONTRACT OR GRANT NUMBER(s)	
Air Force Geophysics Laboratory (LYU) Hanscom AFB Massachusetts 01731			
10. PROGRAM ELEMENT, PROJECT, TASK AREA & WORK UNIT NUMBERS		11. REPORT DATE	
62101F 66781004		14 September 1979	
11. CONTROLLING OFFICE NAME AND ADDRESS		12. NUMBER OF PAGES	
Air Force Geophysics Laboratory (LYU) Hanscom AFB Massachusetts 01731		42	
14. MONITORING AGENCY NAME & ADDRESS (if different from Controlling Office)		15. SECURITY CLASS. (of this report)	
		Unclassified	
		15a. DECLASSIFICATION/DOWNGRADING SCHEDULE	
16. DISTRIBUTION STATEMENT (of this Report)			
Approved for public release, distribution unlimited.			
17. DISTRIBUTION STATEMENT (of the abstract entered in Block 20, if different from Report)			
18. SUPPLEMENTARY NOTES			
19. KEY WORDS (Continue on reverse side if necessary and identify by block number)			
Slant visual range Stochastic process Runway visual range REEP Forward scatter meter Equivalent Markov Weather test facility Markov			
20. ABSTRACT (Continue on reverse side if necessary and identify by block number)			
Analysis of remote tower forward scatter meter measurements of extinction coefficient collected at the Air Force Geophysics Laboratory Weather Test Facility at Otis AFB, Massachusetts demonstrated the accuracy of a remote tower slant visual range (SVR) system. This report describes the final phase of the development and evaluation of a tower SVR system in which the remote tower approach has been extended to include Category I operations. Tests give additional evidence that the runway visual range (RVR) measurements are often not representative of pilot visibility during approach and			

DD FORM 1 JAN 73 1473 EDITION OF 1 NOV 65 IS OBSOLETE

Unclassified
SECURITY CLASSIFICATION OF THIS PAGE (When Data Entered)

4.1.77

4.1

Unclassified

SECURITY CLASSIFICATION OF THIS PAGE(When Data Entered)

Abstract (Continued)

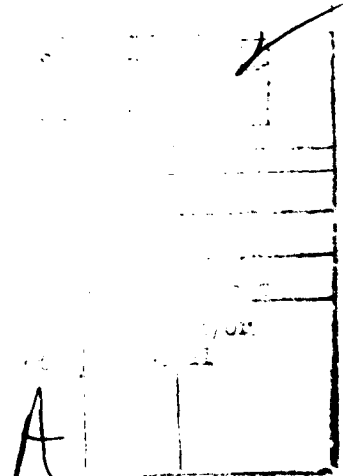
touchdown. An examination of three short range prediction techniques for forecast times of 2, 5, 10, 30 and 60 minutes revealed that the Equivalent Markov technique provides accurate and reliable forecasts of below-limit SVR conditions and yields slightly better results than the Markov and REEP techniques.

Unclassified

SECURITY CLASSIFICATION OF THIS PAGE(When Data Entered)

Preface

This work has benefited from the help of many people without whom successful completion would not have been realized. The author is especially grateful to Donald Chisholm and William Tahnk for many helpful discussions on the development of short-range prediction techniques; Leo Jacobs, Ralph Hoar and Clyde Lawrence, for maintaining the field test instrumentation; Russell Dengel and Joan Ward, for assisting with the data processing; and to Karen Sullivan, for typing the manuscript.



Contents

1. INTRODUCTION	9
2. TEST FACILITY AND DATA SETS	10
3. SLANT VISUAL RANGE SPECIFICATION	13
3.1 Category II	13
3.2 Category I	14
4. PREDICTION TECHNIQUES	17
4.1 Markov Model	17
4.2 Regression Estimation of Event Probabilities (REEP)	19
4.3 Equivalent Markov Model Based on REEP	21
5. EVALUATION CRITERIA	24
6. RESULTS: PREDICTION TECHNIQUES	24
7. CONCLUSIONS	31
REFERENCES	33
APPENDIX A: Method of Calculating Statistics Used in Text	35
APPENDIX B: REEP Technique Equations	37
APPENDIX C: Transition Matrices	41

Illustrations

1. Configuration of Instrumented Towers and Location of FSM Instruments at the AFGL WTF for SVR Tests	12
2. One Minute Average Values of Extinction Coefficient as Measured at Tower A for Pre-Frontal Showers on 14 October 1978	12
3. One Minute Average Values of Extinction Coefficient as Measured at Tower A for Advection Fog on 14 October 1978	13
4. One Minute Average Values of ASVR100, ASVR100 and RVR for Advection Fog on 14 October 1978	15
5. One Minute Average Values of ASVR200, ASVR200 and RVR for Advection Fog on 14 October 1978	16
6. Reliability Graph for Category I Operations: Equivalent Markov Technique: 10 Minute Forecast	26
7. Reliability Graph for Category I Operations: Markov Technique: 10 Minute Forecast	26
8. Reliability Graph for Category I Operations: REEP Technique: 10 Minute Forecast	27
9. Reliability Graph for Category I Operations: Equivalent Markov Technique: 30 Minute Forecast	27
10. Reliability Graph for Category I Operations: Equivalent Markov Technique: 60 Minute Forecast	28
11. Reliability Graph for Category II Operations: Equivalent Markov Technique: 10 Minute Forecast	28
12. Reliability Graph for Category II Operations: Markov Technique: 10 Minute Forecast	29
13. Reliability Graph for Category II Operations: REEP Technique: 10 Minute Forecast	29
14. Reliability Graph for Category II Operations: Equivalent Markov Technique: 30 Minute Forecast	30
15. Reliability Graph for Category II Operations: Equivalent Markov Technique: 60 Minute Forecast	30

Tables

1. Statistical Results of ASVR100 and RVR as Specifiers for ASVR100	15
2. Statistical Results of EST1, EST2 and RVR as Specifiers for ASVR200	16
3. REEP Predictand Category Limits	20
4. REEP Predictor Category Limits	20

Tables

5. Values of Percent Improvement of P-Score for Equivalent Markov and Variation	23
6. Values of P-Score Category I Operations Equivalent Markov, Markov and REEP Techniques	25
7. Values of P-Score Category II Operations Equivalent Markov, Markov and REEP Techniques	31
A1. Contingency Table for Independent Data Set Which Illustrates Method Computing Verification Scores	36

Development and Evaluation of a Tower Slant Visual Range System

1. INTRODUCTION

Improved airfield low-visibility capabilities are being achieved through the installation of advanced instrument landing systems at military and civilian airports. With these advances, the requirement for improved accuracy in prediction techniques for airfield below-limit conditions becomes more prominent. Given a reliable forecast technique, the operational capacity of an airfield can be optimized and extended to include Category IIIa and IIIb landings.

The Federal Aviation Administration (FAA)¹ provides a definition of Slant Visual Range (SVR). Under daylight conditions, SVR is the greater of the slant distance to (1) the farthest high-intensity runway edge light or approach light which a pilot can see at decision height (DH) on the approach path, or (2) the slant distance which would have a transmittance of 5.5 percent. Under conditions of darkness, SVR is the slant distance to the farthest high-intensity runway edge light or approach light which a pilot will see at DH on the approach path. The requirement for a glideslope slant visual range determination and short-range prediction capability exists within the USAF operating commands. Specifically, this report will

(Received for publication 13 September 1979)

1. Bradley, G.S., Lohkamp, C.W., and Williams, R.W. (1976) Flight Test Evaluation of Slant Visual Range/Approach Light Contact Height (SVR/ALCH) Measurement System, Final Report Phase III, FAA-RD-76-167.

will address this scenario for Category I (DH:200 feet, Runway Visual Range: 2600 feet) and Category II (DH:100 feet, Runway Visual Range: 1200 feet) landing operations.

The objective of this study is to develop a statistically based short-range prediction technique which yields probability estimates of below-limit SVR conditions. The approach taken relies on the use of atmospheric extinction coefficient measurements on a tower offset to the side of the landing zone similar in concept to a system proposed by the FAA and originally tested by Bradley, et al.¹ In a preliminary analysis, Hering and Geisler² demonstrated the importance of measurements above ground level for a meaningful description of visibility conditions in support of aircraft landing operations. Measurements aloft up to DH were shown to be of special importance in coastal advection fog conditions since the visibility along the elevated glide slope is predominately lower than indicated by surface runway visual range (RVR) measurements.

This report documents the final phase of the development and evaluation of a tower SVR system by AFGL in which the remote tower approach has been extended to include Category I operations. Three prediction techniques to yield probability estimates of below-limit SVR conditions have been evaluated and comparisons made to determine their respective accuracy and reliability. The first technique, Markov, is an application of the Ornstein-Uhlenbeck process. The second technique, REEP (Regression Estimation of Event Probabilities), is a multiple regression analysis of a dichotomous response variable on dichotomous independent variables. The third technique, Equivalent Markov, is based on a classical Markov transition matrix whose powers are used to prepare forecasts for n-time steps in the future. In the latter two techniques, probability estimates are direct outputs conditioned on the observed SVR. In the Markov technique, the observed SVR must be transformed into an equivalent normal deviate before the probabilities can be computed. Forecast times examined in this study are 2, 5, 10, 30 and 60 minutes.

2. TEST FACILITY AND DATA SETS

The development and testing of a SVR system are a part of the field experiments at the Air Force Geophysics Laboratory (AFGL) Weather Test Facility (WTF) at Otis AFB, Massachusetts. The SVR technique development is also part of a

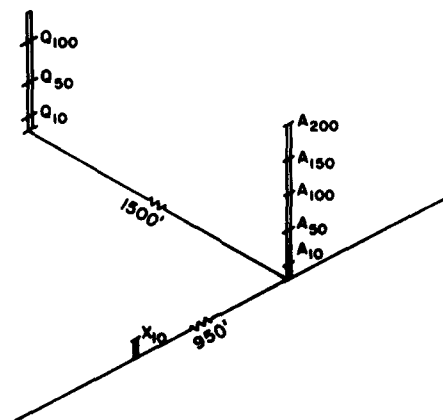
2. Hering, W.S. and Geisler, E.B. (1978) Forward Scatter Meter Measurement of Slant Visual Range, AFGL-TR-78-0191, AD A064 429.

continuing program to upgrade the Modular Automated Weather System (MAWS)³ developed by AFGL for fixed base Air Force requirements.

Measurements of atmospheric extinction coefficient were obtained from forward scatter meters (FSMs) mounted on three towers (A, Q and X) in the AFGL WTF. Figure 1 shows the configuration of the instrumented towers and the heights at which the FSMs were mounted. The FSM instruments (built for the Air Force by EG&G) have been used successfully in several visibility experiments carried out by the AFGL over the past several years. Analysis of the performance characteristics of the FSM for the measurement of extinction coefficient and sensor equivalent visibility are given by Muench⁴ and Chisholm and Jacobs.⁵

The WTF is located in the Cape Cod area where low visibility episodes are predominantly caused by heavy advection fog accompanied by light rain or drizzle. Data are collected at a rate of five observations per minute and are placed on magnetic tape. Subsequent processing yields a time series of one-minute averages of extinction coefficient for each sensor. The continuous data stream from August 1977 to April 1979 was evaluated to identify reduced visibility episodes. This examination revealed a characteristic difference between the SVR and RVR measurements during periods of advection fog and rain of moderate or greater intensity. Figures 2 and 3, acquired in October 1978, clearly depict this. A pre-frontal band of showers passed over the Cape Cod area and by 2230 GMT, heavy advection fog dominated. Note that during periods of moderate rain, the vertical gradient of extinction coefficient (10^{-1} km^{-1}) is nearly zero. During the advection fog period, however, there is a significant increase of extinction coefficient (10^{-1} km^{-1}) with height. SVR specification equations developed from a single data set of these two types of low-visibility episodes could reduce the probability of detecting a below-limit condition of SVR. That is, a systematic bias towards the RVR measurement would result. In order to remove this systematic bias, the selection of low visibility episodes was restricted to the advection fog type. Episodes were selected by applying the criterion that the SVR in the landing zone (tower A) was 1 km^{-1} or more for a period of an hour or greater. Given the universally accepted relationships of extinction coefficient to visibility, a value of 1 km^{-1} corresponds to 1.8 nm using daytime conditions (Koschmieder's Law) and 3.8 nm at night (Allard's Law).

3. Tahnk, W.R. and Lynch, R.H. (1978) The Development of a Fixed Base Automated Weather Sensing and Display System, AFGL-TR-78-0009, AD A054 805.
4. Muench, H.S., Moroz, E.Y., and Jacobs, L.P. (1974) Development and Calibration of the Forward Scatter Visibility Meter, AFCRL-TR-74-0145, AD 783 270.
5. Chisholm, D.A. and Jacobs, L.P. (1975) An Evaluation of Scattering-Type Visibility Instruments, AFCRL-TR-75-0441, AD A016 766.



INSTRUMENT ARRAY FOR
SLANT VISUAL RANGE TESTS

Figure 1. Configuration of Instrumented
Towers and Location of FSM Instruments
at the AFGL WTF for SVR Tests

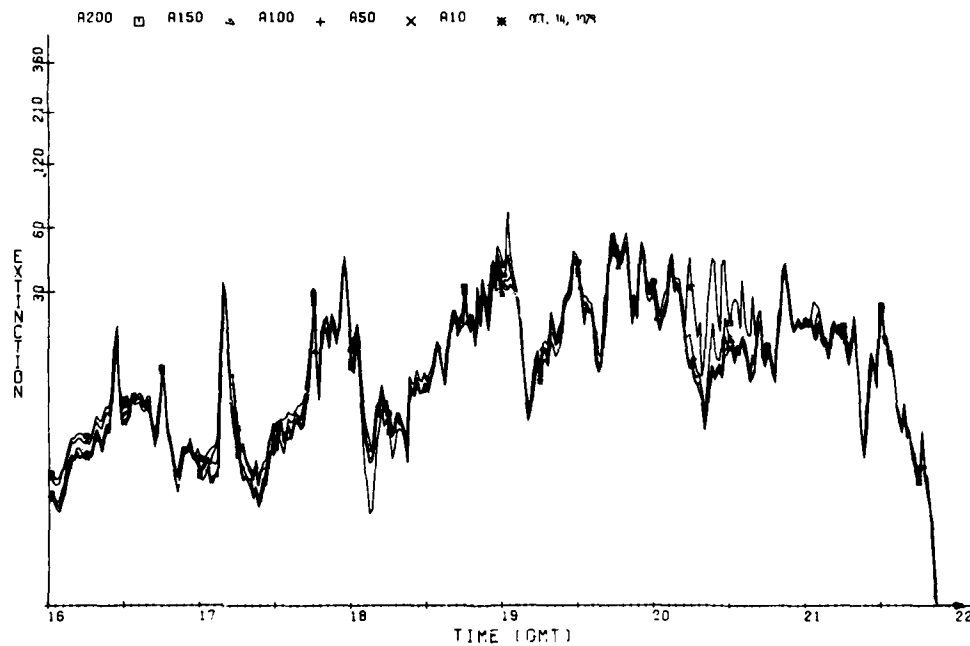


Figure 2. One Minute Average Values of Extinction Coefficient as Measured at
Tower A for Pre-Frontal Showers on 14 October 1978

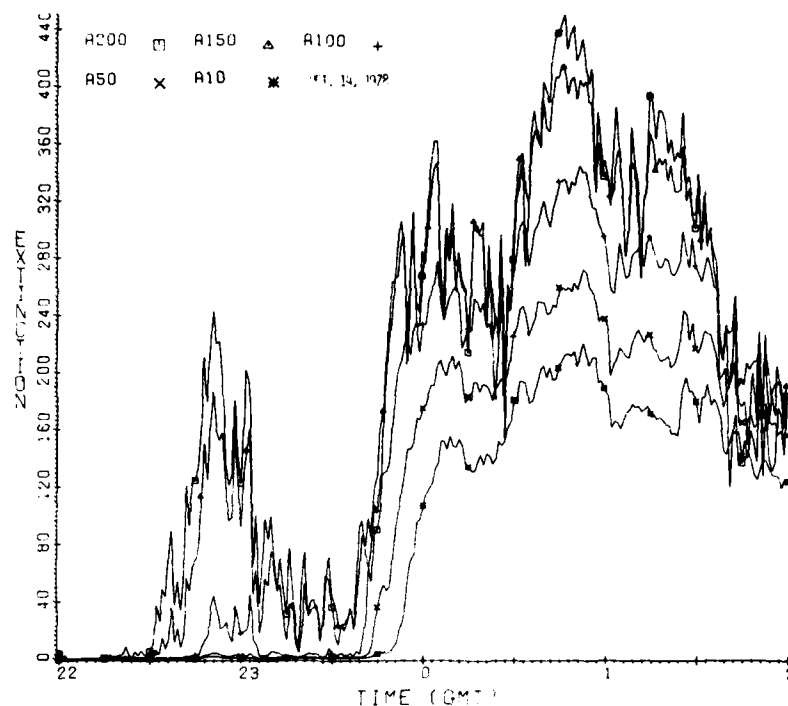


Figure 3. One Minute Average Values of Extinction Coefficient as Measured at Tower A for Advection Fog on 14 October 1978

SVR specification and prediction equations were derived from a dependent data set which consisted of twenty reduced visibility episodes and which contained in excess of 6300 minutes of data. The independent data set, used to test and compare the various techniques, was drawn from twenty-five other episodes totalling over 9900 minutes of reduced visibility.

3. SLANT VISUAL RANGE SPECIFICATION

3.1 Category II

In the report on the first phase of this study (Hering and Geisler²), the accuracy of FSM measurements as specifiers of SVR under Category II conditions was demonstrated. Those results also indicated that during advection fog conditions observed at Cape Cod, a 50 ft remote tower system yields SVR estimates nearly as accurate as a 100 ft remote tower system in which point visibility measurements are made at the same height as the Category II DH.

The earlier study, applicable to Category II conditions, sought to compare the ability of a method which used remote tower measurements of visibility to specify approach zone SVR (ASVR100) to a method which relies on the touchdown RVR measurement. Table 1 summarizes the relevant statistics for the tower option which relies on measurements at 50 ft (referred to as Method 2 in reference 2), identified here as ASVR100, and the control technique (RVR). The threshold 5 km^{-1} corresponds to about 1.2 mile (800 m) daytime visibility and 1 mile (1600 m) at night. The threshold 12 km^{-1} corresponds to 1/4 mile (400 m) daytime and 1/2 mile (800 m) at night. Appendix A describes the method of calculating the statistics used here. Clearly, ASVR100 yields superior specifications of ASVR100 than does RVR. Figure 4, which is a time series plot of an advection fog episode in October 1978, demonstrates that the major deficiency of the RVR method lies in the persistent optimism it conveys to the pilot at DH of seeing his reference point. Recall that lower extinction coefficient values reflect higher visibility.

3.2 Category I

The measurement of SVR to 200 feet was made possible with the installation of FSMs on tower A at the 150 and 200 ft levels. The objective here is to develop a specification equation for SVR of 200 feet (ASVR200) in the simulated approach zone using FSM measurements of extinction coefficient taken at towers Q and X. The FSM measurements at discrete points in the vertical are converted to a weighted vertical average which is used to represent SVR in the approach zone through:

$$\text{ASVR200} = (\text{A200} + 2\text{A150} + 2\text{A100} + 2\text{A50} + \text{A10}) / 8 \quad (1)$$

Application of the multiple linear regression technique to the dependent data set of 6336 observations of reduced visibility yielded two equations for specifying approach zone SVR (ASVR200). The first equation specifies ASVR200 from remote tower (Q100 and Q50) and touchdown RVR (X10) measurements of extinction coefficient as follows:

$$\text{EST1} = \text{Q100} + 0.86\text{X10} - 0.61\text{Q50} \quad (2)$$

The second equation specifies ASVR200 from remote tower (Q50) and touchdown RVR (X10) measurements of extinction coefficient as follows:

$$\text{EST2} = 1.06\text{Q50} + 0.547\text{X10} \quad (3)$$

The second equation (EST2) was developed to measure the loss in skill (if any) which would be experienced if only a 50 ft. offset tower could be utilized.

Table 1. Statistical Results of ASVR100 and RVR as Specifiers for ASVR100

Statistic	ASVR100	RVR
Correlation Coefficient	0.979	0.966
Per cent RMSE	25.4	40.0
Bias	0.4	-37.9
Threshold: 5 km ⁻¹		
TS	90	71
POD	93	71
FAR	3	0
Threshold: 12.0 km ⁻¹		
TS	87	47
POD	92	47
FAR	5	0

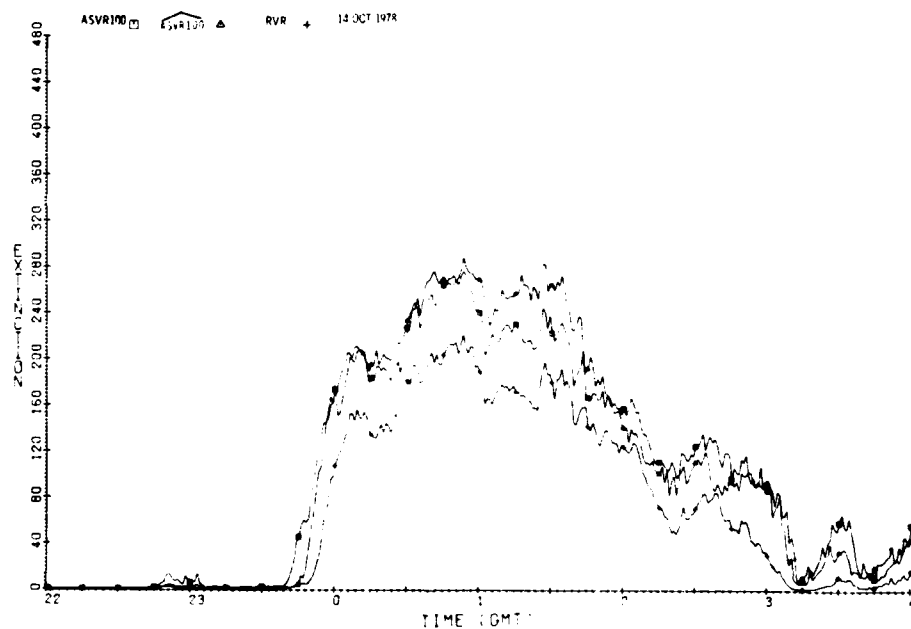


Figure 4. One Minute Average Values of ASVR100, ASVR100 and RVR for Advection Fog on 14 October 1978

Table 2. Statistical Results of EST1, EST2 and RVE as Specifiers for ASVR200

Statistic	EST1	EST2	RVR
Correlation Coefficient	0.971	0.931	0.899
Per cent RMSE	30.8	44.1	58.9
Bias	-5.6	-11.2	-82.9
Threshold: 5 km ⁻¹			
TS	89	68	55
POD	91	69	55
FAR	2	1	0
Threshold: 12 km ⁻¹			
TS	87	70	32
POD	91	71	32
FAR	5	1	0

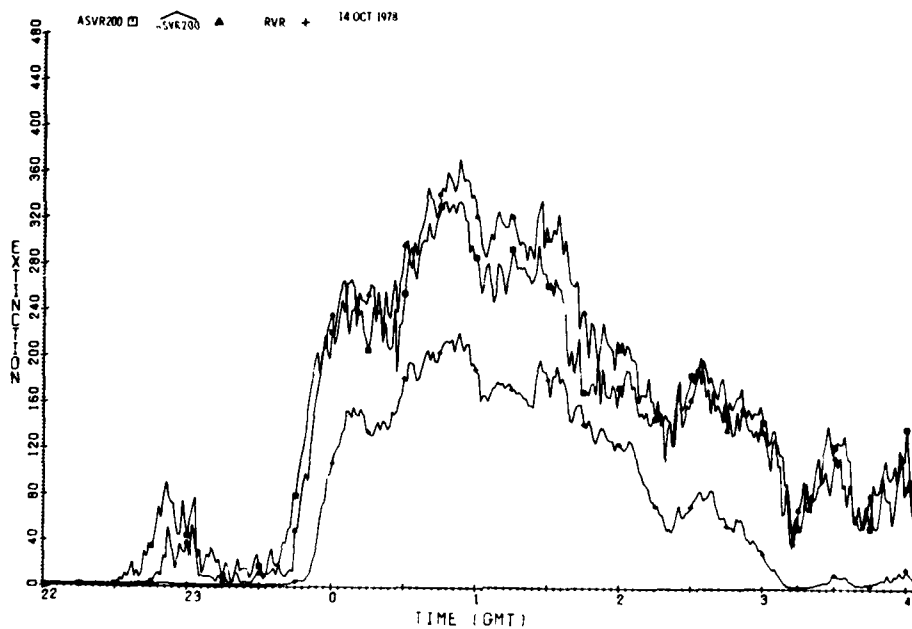


Figure 5. One Minute Average Values of ASVR200, ASVR200 and RVR for Advection Fog on 14 October 1978

Table 2 summarizes the relevant statistics for these specification equations and the control technique (touchdown RVR).

Unlike the results under Category II conditions, the statistics of Category I conditions show that the 100 ft method (EST1) outperforms the 50 ft method (EST2) by nearly 15 percentage points in the RMSE. Similar differences exist in the other statistics. Again we find the remote tower equations are superior to the touchdown RVR measurement. To demonstrate these results we select ASVR200, RVR and ASVR200 (redesignated EST1) and display them in a time series of an advection fog episode in Figure 5. Note the stubborn bias of the RVR measurement while ASVR200 closely tracks ASVR200.

4. PREDICTION TECHNIQUES

4.1 Markov Model

Gringorten⁶ adapted for meteorological use a special class of the Markov chain called the Ornstein-Uhlenbeck process in which a single continuous variate serves as both predictor and predictand (through a time lag). Hering and Quick⁷ used this model with good success in forecasting atmospheric extinction coefficient in the AFGL Mesonet experiments. This model was also used as a control technique in the evaluation of more complex forecasting techniques appropriate for radiation fog (Tahnk⁸) and advective situations (Chisholm⁹).

In the Ornstein-Uhlenbeck stochastic process, the value S_t of the continuous variate at time t is related to an initial value S_0 as follows:

$$S_t = S_0 \rho_0^t + [1 - (\rho_0^t)^2]^{1/2} p \quad (4)$$

where ρ_0 = one hour autocorrelation coefficient; t = forecast time interval (hours);
 p = normalized probability.

6. Gringorten, I.I. (1972) Conditional probability for an exact noncategorized initial condition, Mon. Wea. Rev. 100:796-798.
7. Hering, W.S. and Quick, D.L. (1974) Hanscom visibility forecasting experiments, Proc. of 5th Conference in Weather Forecasting and Analysis, American Meteorological Society, pp. 224-227.
8. Tahnk, W.R. (1975) Objective Prediction of Fine Scale Variations in Radiation Fog Intensity, AFCRL-TR-75-0269, AD A014 774.
9. Chisholm, D.A. (1976) Objective Prediction of Mesoscale Variations of Sensor Equivalent Visibility During Advection Situations, AFGL-TR-76-0132, AD A030 332.

During the AFGL Mesonet network experiment, ρ_o was evaluated in an effort to increase the accuracy of the model when using high-frequency (one-minute) observations. The evaluation yielded seasonal values of $\rho_o = 0.96$ for the period November to March and $\rho_o = 0.93$ from April to October.

S_o is determined in the following way:

$$S_o = k(\ln SVR_o) + 1 \quad (5)$$

where

$\ln SVR_o$ = Slant Visual Range (Extinction Coefficient) at time t_o in logarithmic form

$k, 1$ = function of time before or after sunrise (Δts) through

$$k = a\Delta ts + b \quad (6)$$

$$1 = c\Delta ts + d \quad (7)$$

where

a, b, c, d = constants and coefficients

Δts = hours away from sunrise .

The unconditional cumulative frequency distribution (cfd) of prevailing visibility defined by the terms a, b, c and d is dependent on season and time of day. They were determined from twenty-three years of hourly observations made by operational observers at Otis AFB's runway adjacent to the AFGL WTF. An assumption is made which equates the cfd of prevailing visibility to the cfd of SVR. This is a necessary assumption because there does not exist a SVR data base to accurately determine its cfd.

SVR_o for Categories I and II conditions were obtained from the regression equations which yield specifications of ASVR200 and ASVR100 respectively. Once determining S_t from S_o and the appropriate ρ_o , one computes the probability of exceeding certain operationally significant thresholds by assuming a Gaussian stochastic process and using an approximation to the normal probability integral.

In summary, the most probable normalized SVR is first determined based on a Markov decay of the initial SVR. Assuming a Gaussian distribution of errors about the most probable SVR, one is able to calculate the probability of exceeding a threshold.

4.2 Regression Estimation of Event Probabilities (REEP)

REEP calculates probabilities of being within categories which can easily be converted into exceedance probabilities. Instead of transforming the initial SVR into a most probable SVR from which an exceedance probability can be found (Markov Model), REEP uses the initial SVR directly.

REEP¹⁰ is similar to a forward screening regression technique where a subset of predictors is selected from a large set of possible predictors. The relationship between the predictand and the selected predictors is a linear function whose coefficients are determined by least squares.

REEP requires that each raw variable be broken down into a set of two or more mutually exclusive and exhaustive categories called dummy variables. The dummy variable categories are assigned a value of 1 if the continuous variable falls within the range of the category limits, or 0 if it is outside the range. Therefore, for any one observation, one dummy variable will be assigned a value of 1 and all of the others will be assigned a value of 0.

The result of the least squares technique is a set of equations one for each predictand category:

$$\begin{aligned} P_1 &= A_{01} + A_{11}X_1 + A_{21}X_2 + \dots + A_{91}X_9 \\ P_2 &= A_{02} + A_{12}X_1 + A_{22}X_2 + \dots + A_{92}X_9 \\ &\vdots \\ P_5 &= A_{05} + A_{15}X_1 + A_{25}X_2 + \dots + A_{99}X_9 \end{aligned} \tag{8}$$

Five predictand category limits were selected to coincide with the thresholds prescribed beforehand and which are listed in Table 3.

Category limits were assigned to each predictor based on the relative frequency distribution of the SVR values in the dependent data set. ASVR200 was used to establish the frequency distribution of the dummy predictors for Category I conditions. Similarly, ASVR100 was used for Category II conditions. The resultant categories for the predictors are listed in Table 4.

REEP is formulated to insure internal consistency among predictand categories such that the sum of probabilities totals unity. This is insured by using

10. Miller, R.G. (1964) Regression Estimation of Event Probabilities, Tech. Rpt. 7411-121, The Travelers Research Center, Inc., Hartford, Conn.

Table 3. REEP Predictand Category Limits

Predictand Category	Predictand SVR Limits (km^{-1})	
	Greater Than or Equal To	Less Than
1	1.0	2.0
2	2.0	5.0
3	5.0	12.5
4	12.5	28.1
5	28.1	80.0

Table 4. REEP Predictor Category Limits

Predictor Category	Predictor SVR Limits (km^{-1})	
	Greater Than or Equal To	Less Than
1	1.0	2.0
2	2.0	3.5
3	3.5	5.0
4	5.0	8.5
5	8.5	12.5
6	12.5	18.5
7	18.5	25.0
8	25.0	40.0
9	40.0	80.0

the same predictor categories for each predictand equation. Each predictand equation yields a probability of occurrence for the category (P_i). REEP prediction equations (for intervals of 2, 5, 10, 30 and 60 minutes) were generated from a randomly selected sub-sample of 3000 observations from the dependent sample. The order of selection of dummy variable predictors and the REEP equation sets are listed in Appendix B.

Conversion of REEP categorical probabilities to the probability of exceeding a threshold is simply made after the P_i , $i = 1, 2, \dots, 5$, are calculated. For

example the probability of SVR being below 1/2 mile daytime (P_3 or greater) given $P_1 = 0.1$, $P_2 = 0.15$, $P_3 = 0.35$, $P_4 = 0.25$ and $P_5 = 0.15$ is

$$P(\text{SVR} < 1/2 \text{ mile day}) = P(\text{SVR} > 5 \text{ km}^{-1}) = P_3 + P_4 + P_5$$

Hence

$$P(\text{SVR} < 1/2 \text{ mile day}) = 0.75 .$$

4.3 Equivalent Markov Model Based on REEP

In principle it is possible to develop a prediction scheme in which SVR changes are modeled as a discrete Markov process with a finite-state space. The classical Markov transition Matrix \bar{M} can be used in preparing forecasts for any number of time steps (n) in the future by using powers of \bar{M} . A prediction method that yields probabilistic forecasts comparable to the classical Markov process but without the necessity of utilizing \bar{M} explicitly has been proposed by Miller.¹¹ Miller proposed using the coefficients from a set of REEP equations to determine the one-step transition matrix. Whiton¹² found this technique to yield results comparable to the classical Markov process but much easier to develop and apply to practical forecasting problems. Hillier and Lieberman¹³ utilize a set of conditional or transition probabilities to define the one-step transition matrix \bar{P} . It is this latter approach that the technique used here is based upon.

The REEP equations provide a conditional probability matrix \bar{P} equivalent to \bar{M} . One assumes that the categories (predictor and predictand) used in REEP form a finite Markov chain (X_i), $i = 1, 2, \dots, 5$. Hence, \bar{P} is a square matrix whose predictor and predictand category limits are those found in Table 3.

The stochastic process (X_i) has the Markovian Property

$$P(X_{t+1} = i \mid X_t = j) = P_{ij} \quad ; \quad i, j = 1, 2, \dots, 5 . \quad (9)$$

The existence of one-step transition probabilities P_{ij} implies that for each i, j and n

11. Miller, R. G. (1968) A Stochastic Model for Real-Time On-Demand Weather Predictions, Proc. 1st Statistical Meteorological Conference, American Meteorological Society, pp. 48-51.
12. Whiton, R. W. (1977) Selected Topics in Statistical Meteorology, AWS-TR-77-273, pp. 7-1 to 7-45 or Chap. 7 Markov Processes.
13. Hillier, F. S. and Lieberman, G. J. (1974) Operations Research, Holden-Day, Inc., pp. 351-369.

$$P(X_{t+n} = i \mid X_t = j) = P(X_n = i \mid X_0 = j) = P_{ij}^{(n)} \quad (10)$$

$P_{ij}^{(n)}$ is the conditional probability that the random variable X , starting in state i , will be in state j after exactly n steps (time units) and is called the n -step transition probability.

Since the $P_{ij}^{(n)}$ are conditional probabilities they must have the properties

$$P_{ij}^{(n)} \geq 0 \quad \text{for all } i, j = 1, 2, \dots, 5 \quad (11)$$

$$\sum_{j=1}^5 P_{ij}^{(n)} = 1 \quad \text{for all } i = 1, 2, \dots, 5 \quad (12)$$

$P^{(n)}$ is defined as the n -step transition matrix whose elements are $P_{ij}^{(n)}$

$$\begin{bmatrix} P_{11}^{(n)} & P_{12}^{(n)} & \dots & P_{15}^{(n)} \\ \vdots & & & \vdots \\ \vdots & & & \vdots \\ \vdots & & & \vdots \\ P_{51}^{(n)} & P_{52}^{(n)} & \dots & P_{55}^{(n)} \end{bmatrix} \quad (13)$$

The Chapman-Kolmogorov equations provide a method for computing these n -step transition probabilities:

$$P_{ij}^{(n)} = \sum_{k=1}^5 P_{ik}^{(v)} P_{kj}^{(n-v)}, \quad \text{for all } i, j, n \text{ and } 1 \leq v \leq n. \quad (14)$$

More generally, it follows that the matrix of n -step transition probabilities can be obtained from the expression:

$$P^{(n)} = \bar{P} \cdot \bar{P} \dots \bar{P} = \bar{P}^n = \bar{P} \bar{P}^{n-1} = \bar{P}^{n-1} \bar{P}. \quad (15)$$

Thus the n -step transition probability matrix can be determined by computing the n th power of one-step transition matrix \bar{P} .

In order to calculate the probability of exceeding a threshold one needs to first pre-multiply \bar{P}^n by the observation matrix \bar{O} :

$$\vec{0} = (0_{11} 0_{12} 0_{13} 0_{14} 0_{15}) \quad (16)$$

where the 0_{ij} category is identical to those listed in Table 3. Having calculated $\vec{0P}^n$ one computes the exceedance probabilities in the same way as in the REEP technique.

In the initial application of the Equivalent Markov model, a two minute one-step transition matrix was utilized to generate predictions for 5 through 60 minutes and comparisons were made to Markov and REEP results. The Equivalent Markov model performed poorly when applied in this way, especially at the longer forecast intervals. In an attempt to rectify this, a variation of the Equivalent Markov technique was developed and tested wherein consideration was given to the use of two separate transition matrices to cover the full range of predictions. For SVR of 100 feet (Category II operations), the best results were obtained with a two minute one-step transition matrix to compute conditional probabilities for forecasts of five minutes or greater. For SVR of 200 feet (Category I operations), a two minute one-step transition matrix is used to compute two and five minute forecasts and a ten minute one-step transition matrix is used to compute forecasts of ten minutes or greater. (The calculation of the five minute forecast is made by calculating a simple average of the four and six minute forecasts.)

Table 5. Values of Percent Improvement of P-Score for Equivalent Markov and Variation

SVR Height (ft)	Forecast Time (min)	Thresholds (mile)		
		1	1/2	1/4
200	5	65	35	49
	10	37	37	36
	30	43	34	-2
	60	33	26	-18
100	5	43	30	62
	10	49	39	62
	30	54	42	53
	60	49	38	44

Table 5 presents the percent improvement in P-score (defined in Section 5) of the refined approach over the original approach when evaluated on the dependent data set. Clearly using two one-step transition matrices is a substantial

improvement over using one matrix and this variation alone will be applied in the rest of the study. The transition matrices can be found in Appendix C.

5. EVALUATION CRITERIA

It is desirable that statements of the probability of a weather event be reliable; that is, over a period of time the event should actually occur with the frequency implied by the probability forecast. It is also desirable that there be resolution in the probabilities; that is, they should be as close to 0 or to 100 as possible when the event does not occur or does occur, respectively.

The P-score as defined by Epstein¹⁴ and Murphy¹⁵ measures these two characteristics of probability forecasts and represents the mean square difference between the forecast and observed probability distribution. It is given by:

$$PS = \frac{1}{N} \sum_{i=1}^N (F_i - O_i)^2 \quad (17)$$

where

F_i = forecast probability of exceeding the threshold

O_i = verification based on observed SVR as follows:

1 = if threshold is exceeded

0 = if not .

The nature of PS is such that it attains a value of 0 with perfect probability forecast (that is, 0 or 100 percent probability and correct) or a value of 1 if totally imperfect (that is, 0 or 100 percent and incorrect).

6. RESULTS: PREDICTION TECHNIQUES

The aviation industry has progressed to the point where a significant number of airfields have been upgraded and approved for Category II operations. As such, this study has focussed on Categories I and II landing conditions. These categories

14. Epstein, E.S. (1969) A scoring system for probability forecasts of ranked categories, J. Appl. Meteorol. 8:985-987.

15. Murphy, A.H. (1969) On the ranked probability score, J. Appl. Meteorol. 8:988-989.

correspond to a daytime SVR threshold of 1/2 mile for Category I and a threshold 1/4 mile for Category II, respectively. The three prediction techniques were applied to each of the twenty-five independent data episodes. The results of each episode were combined to reflect the overall accuracy and reliability of each prediction technique. Comparison of the three techniques was achieved by use of the P-score statistic which calculates the mean squared probability error and by reliability graphs.

Verification results of the P-score for Category I operations given in Table 6 reflect that the Equivalent Markov technique yields a slight improvement over the Markov and REEP techniques (2 percent and 9 percent respectively). Figures 6 to 8 depict the reliability of the three techniques for 10 min predictions. Clearly the predicted probabilities of the Equivalent Markov and REEP techniques are quite close to the observed frequencies. However, the predicted probabilities of the Markov technique tend to underestimate the observed frequencies.

Figures 9 and 10 reveal a slight tendency of the Equivalent Markov technique to overestimate below limit SVR conditions for Category I operations for forecast times of 30 to 60 minutes, respectively.

Table 7 summarizes the results for Category II operations. The Equivalent Markov technique yields systematically better P-scores over the Markov and REEP techniques. Figures 11 and 13 show the excellent correspondence between the predicted probabilities and the observed frequencies for the Equivalent Markov and REEP techniques. Meanwhile, Figure 12 reflects the tendency of the Markov technique to overestimate the observed frequencies. A dropoff in skill of the Equivalent Markov technique, as the forecast interval is increased from 10 to 60 minutes, is due in part to decreasing resolution in the low probability forecasts. This can be seen in Figures 11, 14 and 15 that show the percentage of forecasts in the 0-5 percent range lowers from 85 to 72 to 58 percent.

Table 6. Values of P-Score Category I Operations
Equivalent Markov, Markov and REEP Techniques

Lag	Prediction Technique		
	Markov	REEP	Equiv-Markov
2	0.046	0.048	0.045
5	0.055	0.060	0.035
10	0.075	0.081	0.074
30	0.131	0.139	0.129
60	0.172	0.196	0.169

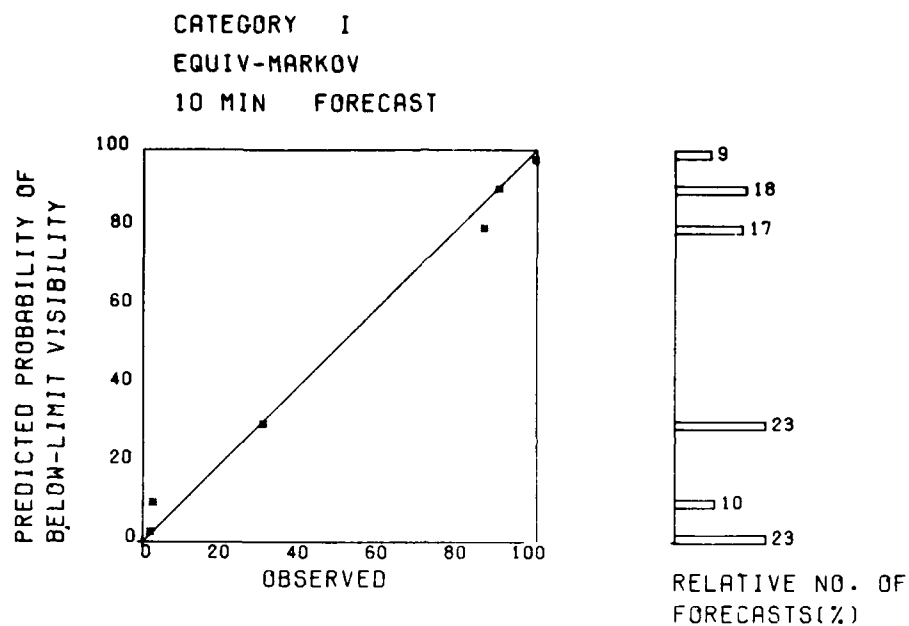


Figure 6. Reliability Graph for Category I Operations:
Equivalent Markov Technique: 10 Minute Forecast

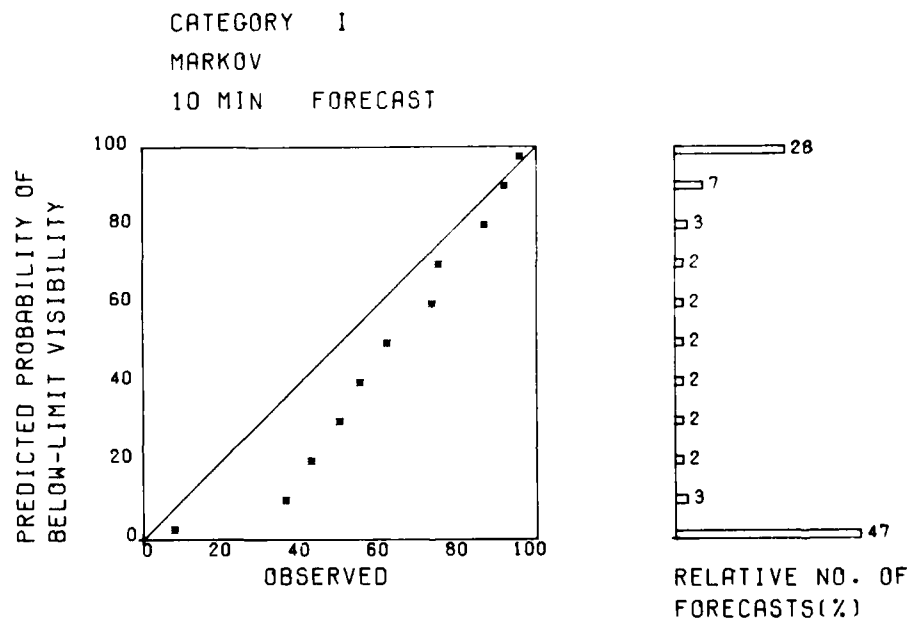


Figure 7. Reliability Graph for Category I Operations:
Markov Technique: 10 Minute Forecast

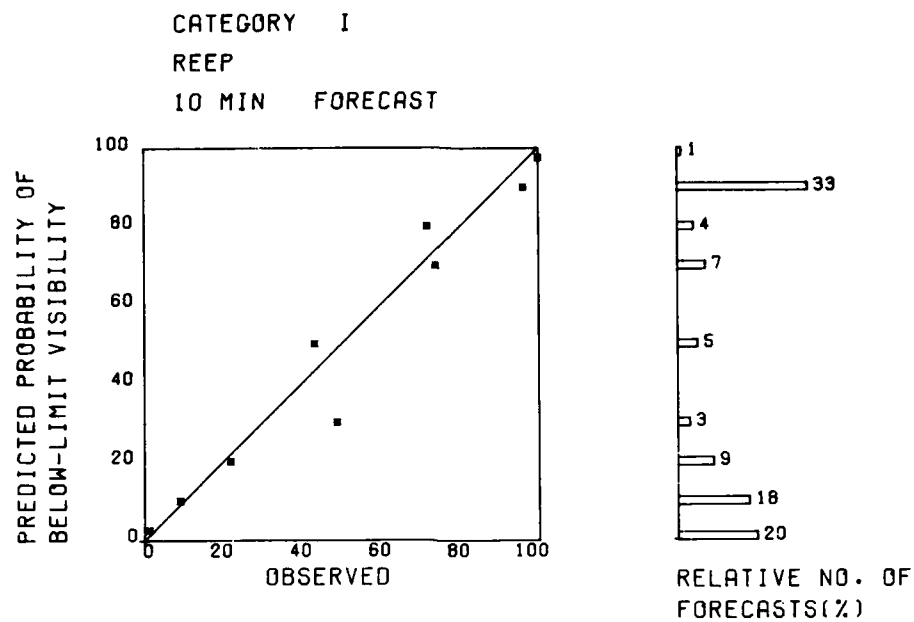


Figure 8. Reliability Graph for Category I Operations:
REEP Technique: 10 Minute Forecast

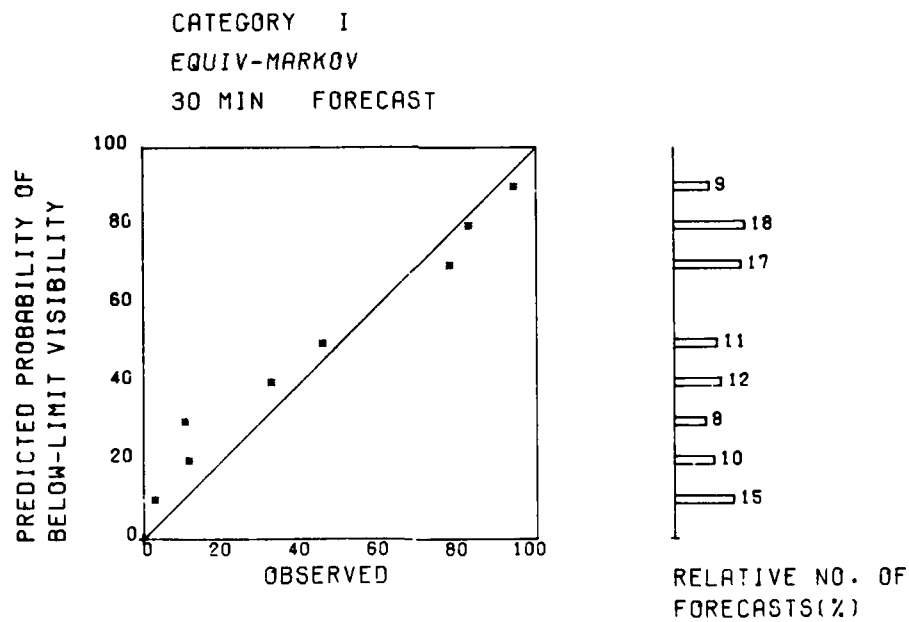


Figure 9. Reliability Graph for Category I Operations:
Equivalent Markov Technique: 30 Minute Forecast

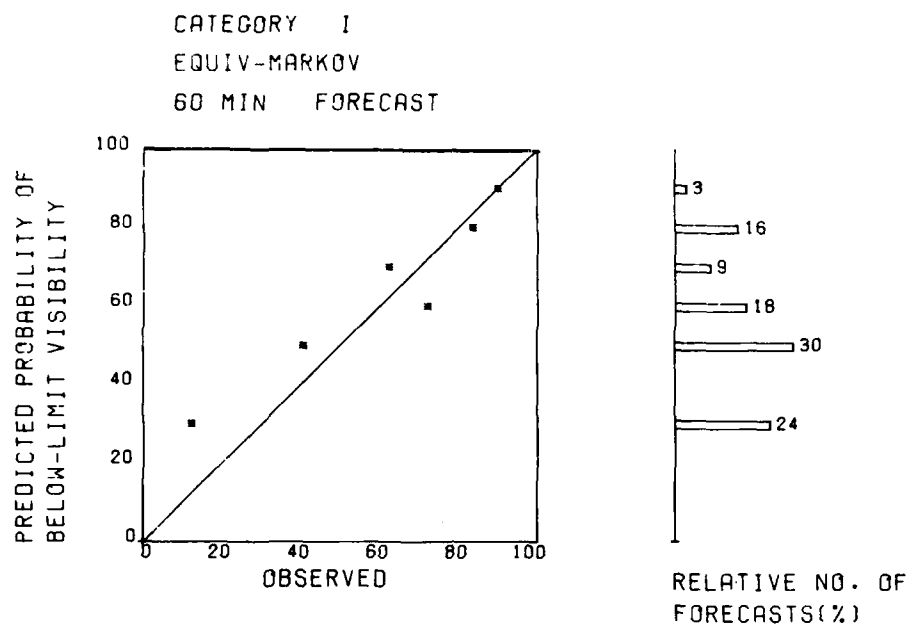


Figure 10. Reliability Graph for Category I Operations:
Equivalent Markov Technique: 60 Minute Forecast

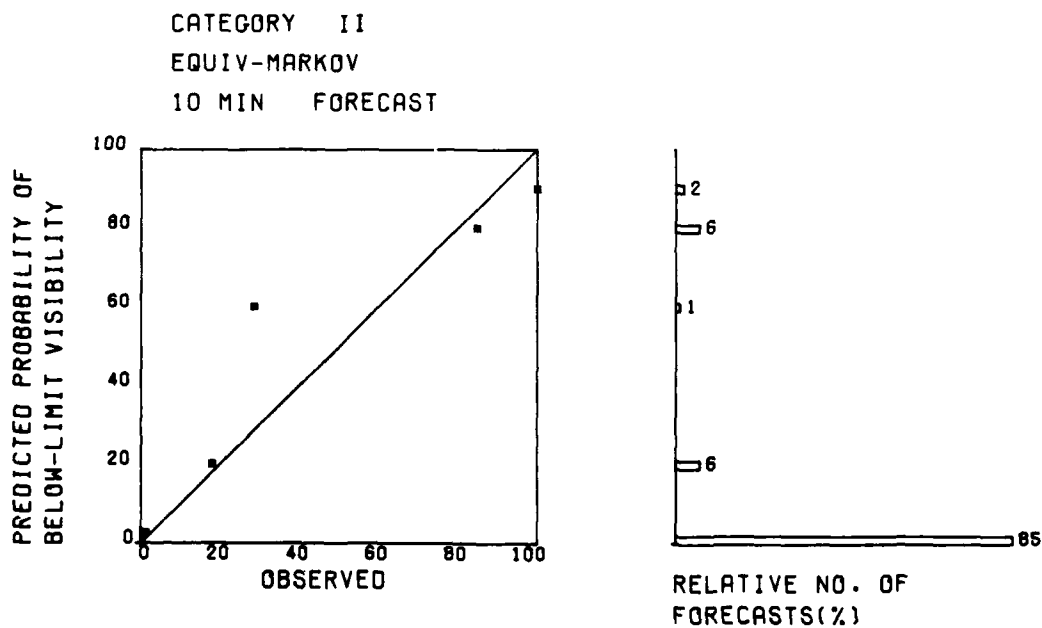


Figure 11. Reliability Graph for Category II Operations:
Equivalent Markov Technique: 10 Minute Forecast

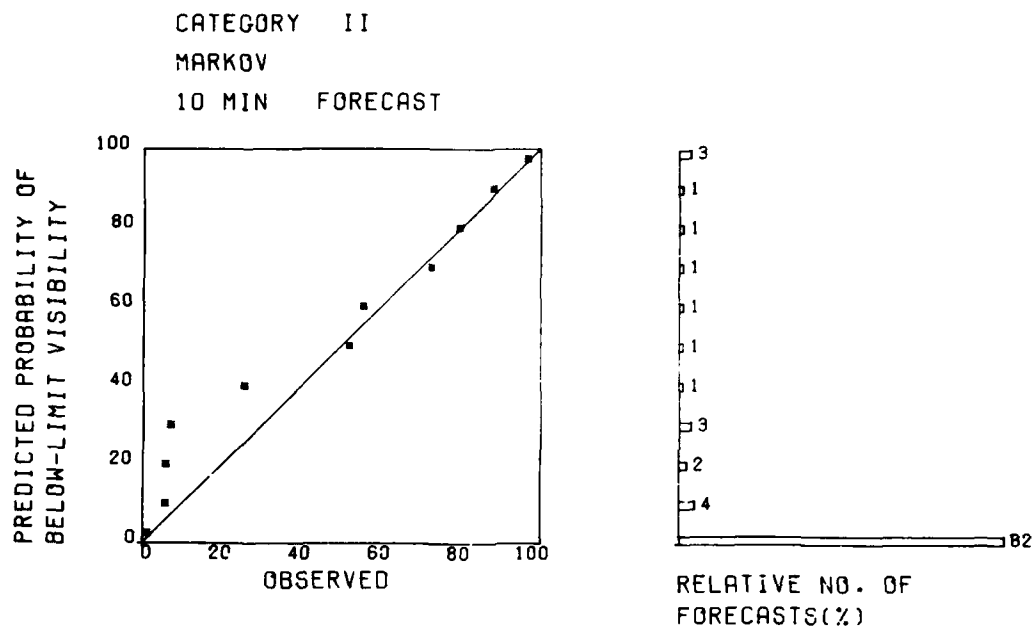


Figure 12. Reliability Graph for Category II Operations:
Markov Technique: 10 Minute Forecast

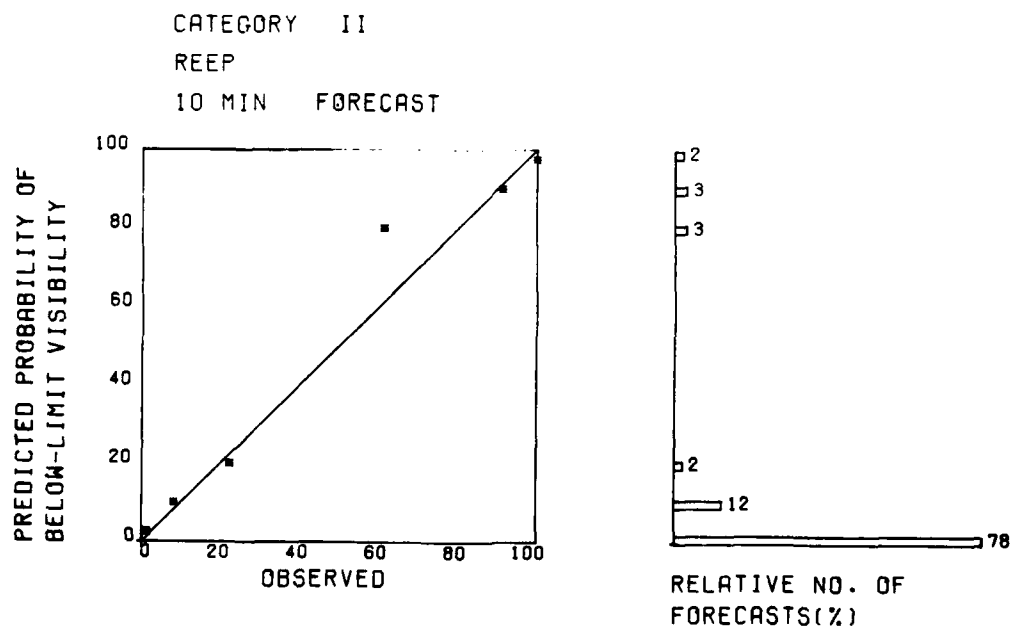


Figure 13. Reliability Graph for Category II Operations:
REEP Technique: 10 Minute Forecast

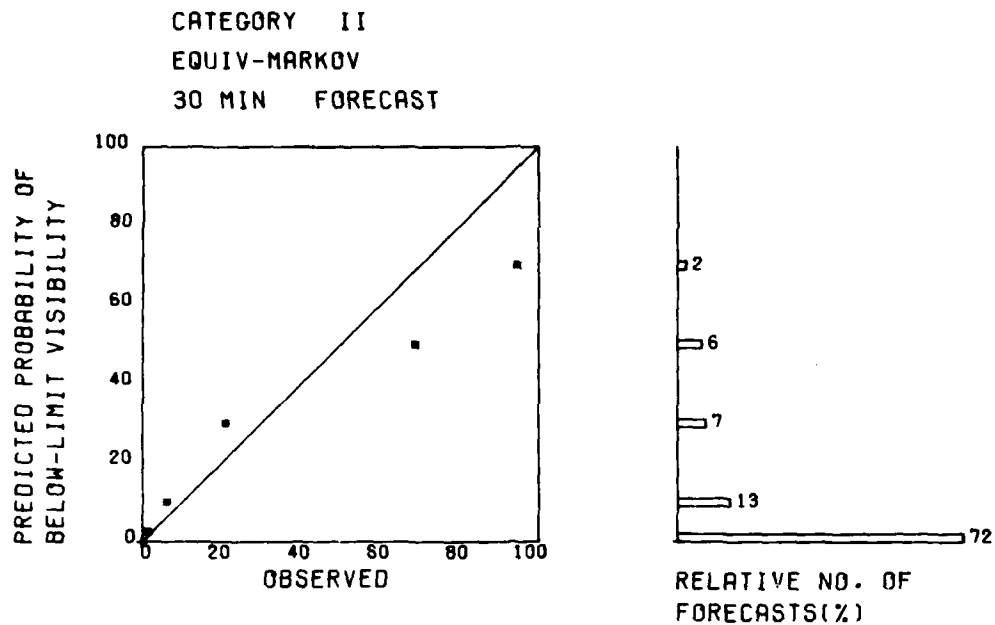


Figure 14. Reliability Graph for Category II Operations:
Equivalent Markov Technique: 30 Minute Forecast

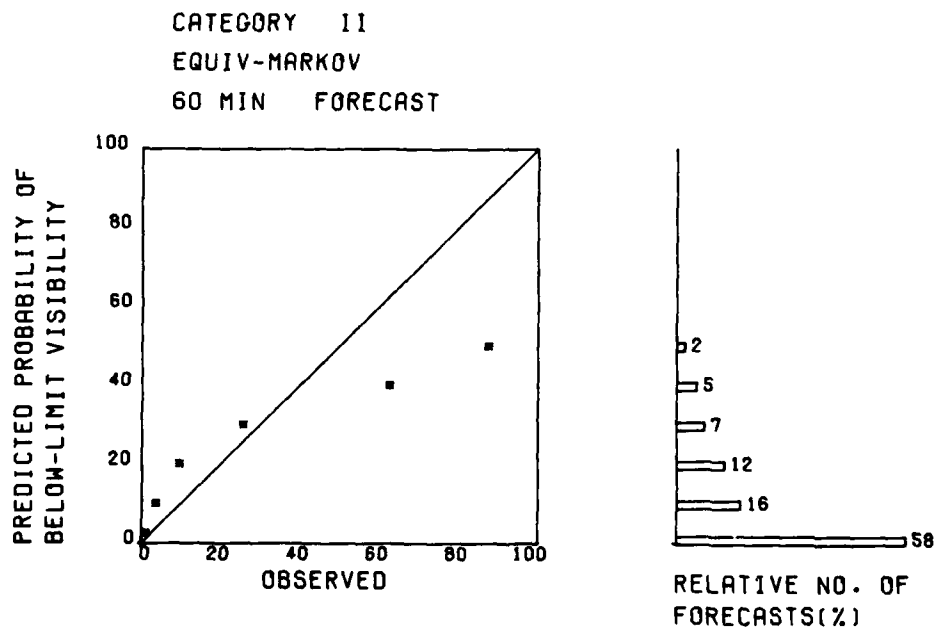


Figure 15. Reliability Graph for Category II Operations:
Equivalent Markov Technique: 60 Minute Forecast

**Table 7. Values of P-Score Category II Operations
Equivalent Markov, Markov and REEP Techniques**

Lag	Prediction Technique		
	Markov	REEP	Equiv-Markov
2	0.018	0.018	0.017
5	0.021	0.019	0.019
10	0.028	0.025	0.024
30	0.052	0.046	0.044
60	0.067	0.056	0.058

It was stated above that the Markov technique underestimates the observed frequencies for Category I conditions and overestimates them for Category II conditions. This probably reflects a weakness in the original assumption of equating the cfd of prevailing visibility to the cfd of SVR, an assumption which had to be made due to the lack of SVR data to determine its cfd directly.

7. CONCLUSIONS

Analysis of the data collected at the AFGL WTF demonstrates the accuracy and reliability of a remote tower SVR system. For both Categories I and II operations such a system would provide a probability of detection of below-limit conditions of 91 percent or greater, a large improvement over using the surface RVR instrument. In an examination of the short range prediction techniques, the Equivalent Markov technique was shown to provide accurate and reliable forecasts of below-limit SVR conditions and yield slightly better results on independent data than did the Markov and REEP technique. Due to the high-frequency fluctuations characteristic of coastal advection fog episodes, a continuous updating and disseminating system is recommended to allow this information to be used in a timely manner. An automated weather system such as MAWS can easily accommodate this feature.

The SVR specification equations (ASVR100 and ASVR200) and the Equivalent Markov technique are being integrated into the MAWS recently installed at the AFGL WTF as part of a continuing investigation of automated airfield weather observation and prediction systems.

References

1. Bradley, G.S., Lohkamp, C.W., and Williams, R.W. (1976) Flight Test Evaluation of Slant Visual Range/Approach Light Contact Height (SVR/ALCH) Measurement System, Final Report Phase III, FAA-RD-76-167.
2. Hering, W.S. and Geisler, E.B. (1978) Forward Scatter Meter Measurement of Slant Visual Range, AFGL-TR-78-0191, AD A064 429.
3. Tahnk, W.R. and Lynch, R.H. (1978) The Development of a Fixed Base Automated Weather Sensing and Display System, AFGL-TR-78-0009, AD A054 805.
4. Muench, H.S., Moroz, E.Y., and Jacobs, L.P. (1974) Development and Calibration of the Forward Scatter Visibility Meter, AFCRL-TR-74-0145, AD 783 270.
5. Chisholm, D.A. and Jacobs, L.P. (1975) An Evaluation of Scattering-Type Visibility Instruments, AFCRL-TR-75-0441, AD A016 766.
6. Gringorten, I.I. (1972) Conditional probability for an exact noncategorized initial condition, Mon. Wea. Rev. 100:796-798.
7. Hering, W.S. and Quick, D.L. (1974) Hanscom visibility forecasting experiments, Proc. of 5th Conference in Weather Forecasting and Analysis, American Meteorological Society, pp. 224-227.
8. Tahnk, W.R. (1975) Objective Prediction of Fine Scale Variations in Radiation Fog Intensity, AFCRL-TR-75-0269, AD A014 774.
9. Chisholm, D.A. (1976) Objective Prediction of Mesoscale Variations of Sensor Equivalent Visibility During Advection Situations, AFGL-TR-76-0132, AD A030 332.
10. Miller, R.G. (1964) Regression Estimation of Event Probabilities, Tech. Rpt. 7411-121, The Travelers Research Center, Inc., Hartford, Conn.
11. Miller, R.G. (1968) A Stochastic Model for Real-Time On-Demand Weather Predictions, Proc. 1st Statistical Meteorological Conference, American Meteorological Society, pp. 48-51.

12. Whiton, R. W. (1977) Selected Topics in Statistical Meteorology, AWS-TR-77-273, pp. 7-1 to 7-45 or Chap. 7 Markov Processes.
13. Hillier, F.S. and Lieberman, G.J. (1974) Operations Research, Holden-Day, Inc., pp. 351-369.
14. Epstein, E.S. (1969) A scoring system for probability forecasts of ranked categories, J. Appl. Meteorol. 8:985-987.
15. Murphy, A.H. (1969) On the ranked probability score, J. Appl. Meteorol. 8:988-989.

Appendix A

Method of Calculating Statistics Used in Text

1. Per Cent Root Mean Square Error (% RMSE)

$$\% \text{ RMSE} = \left[\frac{1}{N} \sum_{i=1}^N \frac{F_i - O_i}{O_i}^2 \right]^{1/2} \times 100$$

where

$$F_i = \widehat{\text{ASVR200}}$$

$$O_i = \text{ASVR200}$$

% RMSE = 0 is perfect

2. Bias

$$\text{BIAS} = \frac{1}{N} \sum_{i=1}^N (F_i - O_i)$$

where

$$F_i = \widehat{\text{ASVR200}}$$

$$O_i = \text{ASVR200}$$

BIAS = 0 is perfect

3. Correlation Coefficient (R)

$$R = \frac{\sum XY}{\sqrt{(\sum X^2)(\sum Y^2)}}$$

where

$$X = (\widehat{\text{ASVR200}} - \overline{\text{ASVR200}})$$

$$Y = (\widehat{\text{ASVR200}} - \overline{\text{ASVR200}})$$

4. Contingency Table

The following data display in Table A1 depicts the accuracy of $\widehat{\text{ASVR200}}$ as a specifier for ASVR200 for a threshold of 5 km^{-1} (day: 1/2 mile; night: 1/2 mile) and a time lag of 0 minutes.

1) Threat Score (TS)

$$TS = (5453 / (6028 + 97)) \times 100 = 89.0\%$$

2) Probability of Detection (POD)

$$POD = (5453 / 6028) \times 100 = 90.5\%$$

3) False Alarm Ratio (FAR)

$$FAR = (97 / 5550) \times 100 = 1.7\%$$

Table A1. Contingency Table for Independent Data Set Which Illustrates Method Computer Verification Scores

Observed	Forecast		
	$SVR \geq 5 \text{ km}^{-1}$	$SVR < 5 \text{ km}^{-1}$	Total Min
Visibility below Limit $SVR \geq 5 \text{ km}^{-1}$	5453	575	6028
Visibility above Limit $SVR < 5 \text{ km}^{-1}$	97	3782	3879
Total Min	5550	4357	9907

Appendix B

REEP Technique Equations

Category I Operations

Two Minute Forecast							
Order (i)	P ₁	P ₂	P ₃	P ₄	P ₅	Predictor Xi	Limits of Xi
0	0	0.100	0.025	0.667	0.198	0	
1	0	-0.096	-0.019	-0.511	0.627	8	25-40
2	0	-0.100	-0.025	-0.671	0.795	9	40-80
3	0.836	0.035	0.005	-0.677	-0.198	1	1-2
4	0.499	0.314	0.058	-0.672	-0.198	2	2-3.5
5	0.033	0.014	0.693	-0.542	-0.198	4	5-8.5
6	0.025	-0.010	0.465	-0.281	-0.198	5	8.5-12.5
7	0.122	0.213	0.515	-0.651	-0.198	3	3.5-5
8	0.019	-0.029	0.082	0.126	-0.198	6	12.5-18.5

Category I Operations (Cont.)

Five Minute Forecast							
Order	P ₁	P ₂	P ₃	P ₄	P ₅	Predictor Xi	Limits of Xi
0	0.008	0.102	0.03	0.644	0.216	0	
1	-0.008	-0.098	-0.021	-0.468	0.595	8	25-40
2	-0.008	-0.102	-0.03	-0.631	0.771	9	40-80
3	0.699	0.132	0.029	-0.644	-0.216	1	1-2
4	0.482	0.304	0.050	-0.620	-0.216	2	2-3.5
5	0.016	0.040	0.655	-0.494	-0.216	4	5-8.5
6	0.017	-0.014	0.419	-0.205	-0.216	5	8.5-12.5
7	0.122	0.194	0.510	-0.609	-0.216	3	3.5-5
8	0.006	-0.011	0.077	0.134	-0.205	6	12.5-18.5

Ten Minute Forecast							
Order	P ₁	P ₂	P ₃	P ₄	P ₅	Predictor Xi	Limits of Xi
0	0.191	0.296	0.374	0.139	0.000	0	
1	-0.191	-0.287	-0.363	0.080	-0.761	8	25-40
2	0.191	-0.296	-0.374	-0.087	0.948	9	40-80
3	0.291	0.069	-0.248	-0.112	0.000	2	2-3.5
4	0.405	-0.032	-0.234	-0.139	0.000	1	1-2
5	-0.149	-0.164	-0.263	0.050	0.000	4	5-8.5
6	-0.185	-0.186	-0.346	-0.435	0.282	7	18.5-25
7	-0.172	-0.230	-0.240	0.606	0.036	6	12.5-18.5
8	-0.157	-0.221	0.075	0.300	0.003	5	8.5-12.5

Thirty Minute Forecast							
Order (i)	P ₁	P ₂	P ₃	P ₄	P ₅	Predictor Xi	Limits of Xi
0	0.053	0.069	0.470	0.364	0.044	0	
1	-0.042	-0.047	-0.446	-0.126	0.661	8	25-40
2	-0.053	-0.069	-0.431	-0.090	0.643	9	40-80
3	-0.033	0.027	-0.433	0.147	0.292	7	18.5-25
4	0.295	0.326	-0.290	-0.299	-0.033	2	2-3.5
5	0.380	0.212	-0.301	-0.248	-0.044	1	1-2
6	-0.031	0.008	-0.295	0.244	0.074	6	12.5-18.5
7	0.164	0.184	-0.131	-0.208	-0.009	3	3.5-5
8	0.043	0.019	0.004	-0.046	-0.020	4	5-8.5

Sixty Minute Forecast							
Order (i)	P ₁	P ₂	P ₃	P ₄	P ₅	Predictor Xi	Limits of Xi
0	0.066	0.093	0.381	0.339	0.120	0	
1	-0.048	-0.060	-0.343	0.003	0.447	8	25-40
2	-0.009	-0.024	-0.327	0.141	0.219	7	18.5-25
3	0.170	0.241	-0.113	-0.197	-0.101	2	2-3.5
4	0.209	0.223	-0.153	-0.211	-0.067	1	1-2
5	0.021	0.211	-0.051	-0.157	-0.024	3	3.5-5
6	-0.007	-0.034	-0.231	-0.026	0.298	9	40-80
7	-0.047	-0.022	-0.138	0.066	0.140	6	12.5-18.5
8	-0.019	0.047	-0.048	-0.056	0.076	5	8.5-12.5

Category II Operations

Two Minute Forecast							
Order (i)	P ₁	P ₂	P ₃	P ₄	P ₅	Predictor Xi	Limits of Xi
0	0.000	0.017	0.869	0.114	0.000	0	
1	0.907	0.075	-0.865	-0.114	0.000	1	1-2
2	0.000	-0.017	-0.869	0.032	0.854	9	40-80
3	0.000	-0.107	-0.855	0.207	0.666	8	25-40
4	0.000	-0.017	-0.817	0.832	0.003	7	18.5-25
5	0.000	-0.017	-0.736	0.753	0.000	6	12.5-18.5
6	0.251	0.688	-0.825	-0.114	0.000	2	2-3.5
7	0.020	0.637	-0.564	-0.114	0.000	3	3.5-5
8	0.019	0.223	-0.141	-0.101	0.000	4	5-8.5

Five Minute Forecast							
Order (i)	P ₁	P ₂	P ₃	P ₄	P ₅	Predictor Xi	Limits of Xi
0	0.000	0.048	0.790	0.162	0.000	0	
1	0.859	0.076	-0.773	-0.162	0.000	1	1-2
2	0.000	-0.048	-0.784	-0.021	0.854	9	40-80
3	0.000	-0.048	-0.776	0.183	0.641	8	25-40
4	0.000	-0.048	-0.722	0.766	0.005	7	18.5-25
5	0.000	-0.048	-0.623	0.672	0.000	6	12.5-18.5
6	0.280	0.583	-0.704	-0.159	0.000	2	2-3.5
7	0.074	0.595	-0.507	-0.162	0.000	3	3.5-5
8	0.028	0.208	-0.099	-0.137	0.000	4	5-8.5

Category II Operations (Cont.)

Ten Minute Forecast							
Order (i)	P ₁	P ₂	P ₃	P ₄	P ₅	Predictor Xi	Limits of Xi
0	0.125	0.588	0.272	0.015	0.000	0	
1	0.674	-0.431	-0.230	-0.013	0.000	1	1-2
2	-0.125	-0.588	-0.251	0.126	0.839	9	40-80
3	-0.125	-0.588	-0.255	0.316	0.652	8	25-40
4	-0.125	-0.578	-0.189	0.866	0.026	7	18.5-25
5	-0.125	-0.585	-0.067	0.775	0.003	6	12.5-18.5
6	-0.115	-0.557	0.424	0.247	0.000	5	8.5-12.5
7	-0.078	-0.219	0.315	0.054	0.000	4	5-8.5
8	0.194	-0.037	-0.145	-0.012	0.000	2	2-3.5

Thirty Minute Forecast							
Order (i)	P ₁	P ₂	P ₃	P ₄	P ₅	Predictor Xi	Limits of Xi
0	0.184	0.371	0.375	0.066	0.044	0	
1	-0.184	-0.371	-0.297	0.054	0.798	9	40-80
2	-0.184	-0.340	-0.278	0.296	0.507	8	25-40
3	0.378	-0.101	-0.258	-0.024	0.005	1	1-2
4	-0.163	-0.361	-0.215	0.650	0.089	7	18.5-25
5	-0.170	-0.360	-0.131	0.618	0.043	6	12.5-18.5
6	-0.125	-0.275	0.118	0.255	0.027	5	8.5-12.5
7	0.158	0.027	-0.166	-0.109	-0.001	2	2-3.5
8	-0.053	-0.109	0.013	0.140	0.009	4	5-8.5

Sixty Minute Forecast							
Order (i)	P ₁	P ₂	P ₃	P ₄	P ₅	Predictor Xi	Limits of Xi
0	0.194	0.209	0.256	0.234	0.106	0	
1	-0.168	-0.209	-0.136	-0.167	0.680	9	40-80
2	0.250	0.066	-0.097	-0.147	-0.072	1	1-2
3	-0.135	-0.085	-0.146	0.110	0.256	8	25-40
4	-0.194	-0.171	-0.062	0.489	-0.062	6	12.5-18.5
5	-0.176	-0.181	-0.044	0.425	-0.024	7	18.5-25
6	-0.125	0.008	0.071	0.104	-0.058	5	8.5-12.5
7	-0.028	-0.015	0.189	-0.102	-0.044	3	3.5-5
8	0.060	0.094	0.024	-0.090	-0.089	2	2-3.5

Appendix C

Transition Matrices

The following one-step transition matrices are used in the equivalent Markov prediction technique and can be interpreted in the following way:

$$P = \begin{bmatrix} P_{11} & P_{12} & \dots & P_{15} \\ P_{21} & P_{22} & \dots & P_{25} \\ \vdots & & & \vdots \\ P_{51} & P_{52} & \dots & P_{55} \end{bmatrix}$$

where

$$P_{ij} = P[SVR_t = i \mid SVR_0 = j] \quad \text{for } i, j, = 1, 2, \dots, 5$$

That is, P_{ij} is the transition or conditional probability that SVR at time t will be in state i given that SVR at time 0 is in state j .

1. Category I Operations

Two-minute one-step transition matrix

$$P = \begin{bmatrix} 0.817 & 0.152 & 0.030 & 0.000 & 0.000 \\ 0.340 & 0.426 & 0.219 & 0.014 & 0.000 \\ 0.025 & 0.091 & 0.623 & 0.260 & 0.000 \\ 0.004 & 0.096 & 0.054 & 0.696 & 0.148 \\ 0.000 & 0.003 & 0.007 & 0.032 & 0.868 \end{bmatrix}$$

Ten-minute one-step transition matrix

$$P = \begin{bmatrix} 0.635 & 0.275 & 0.092 & 0.000 & 0.000 \\ 0.402 & 0.318 & 0.234 & 0.047 & 0.000 \\ 0.034 & 0.093 & 0.594 & 0.277 & 0.003 \\ 0.011 & 0.096 & 0.068 & 0.629 & 0.197 \\ 0.000 & 0.007 & 0.013 & 0.171 & 0.810 \end{bmatrix}$$

2. Category II Operations

Two-minute one-step transition matrix

$$P = \begin{bmatrix} 0.906 & 0.083 & 0.010 & 0.000 & 0.000 \\ 0.178 & 0.624 & 0.198 & 0.000 & 0.000 \\ 0.005 & 0.128 & 0.804 & 0.063 & 0.000 \\ 0.000 & 0.000 & 0.104 & 0.891 & 0.005 \\ 0.000 & 0.000 & 0.015 & 0.232 & 0.753 \end{bmatrix}$$

Five-minute one-step transition matrix

$$P = \begin{bmatrix} 0.838 & 0.140 & 0.023 & 0.000 & 0.000 \\ 0.207 & 0.574 & 0.216 & 0.003 & 0.000 \\ 0.011 & 0.138 & 0.750 & 0.100 & 0.000 \\ 0.000 & 0.002 & 0.130 & 0.861 & 0.008 \\ 0.000 & 0.000 & 0.018 & 0.219 & 0.763 \end{bmatrix}$$